Journal of Applied Mechanics and Technical Physics, Vol. 47, No. 3, pp. 366–376, 2006

DIFFERENTIAL CHARACTERISTICS OF THE FLOW FIELD IN A PLANE OVEREXPANDED JET IN THE VICINITY OF THE NOZZLE LIP

V. N. Uskov and M. V. Chernyshov

UDC 533.6.011.72

A method of theoretical investigation of the flow field in a two-dimensional (plane–parallel or axisymmetric) overexpanded jet of an ideal perfect gas in the vicinity of the nozzle lip is described. The changes in curvature of the shock wave emanating from the lip, as well as the shock-wave intensity and flow parameters behind the shock are analyzed as functions of the Mach number, pressure ratio in the plane jet, and ratio of specific heats of the gas.

Key words: *supersonic overexpanded jet, shock-wave curvature, jet boundary, compressed layer.*

Introduction. Governing Relations. Many properties of a supersonic jet of a gas are determined by the specific features of its flow in the vicinity of the nozzle exit (nozzle lip). For instance, the initial curvature of the boundary of an axisymmetric jet is responsible for the development of streamwise Taylor–Görtler vortices [1–6], the shape of the incident shock wave determines the flow vorticity in the compressed layer behind the shock wave, and the boundary-layer separation from the nozzle walls can be predicted by analyzing the properties of the shock emanating from the nozzle lip and from the jet boundary in an inviscid flow.

The curvature of the shock emanating from the nozzle lip during the exhaustion of a plane overexpanded jet is theoretically considered in the present paper on the basis of differential equations of dynamic compatibility [7]. This quantity is shown to be an important parameter of the problem, used to analyze the changes in shock-wave intensity, Mach number, static and total pressures in the compressed layer behind the shock wave, and curvature of the jet boundary in the vicinity of the nozzle lip. The study is performed in a wide range of the basic parameters of the overexpanded jet of an inviscid perfect gas.

An overexpanded jet exhausted into the ambient space is characterized by the jet pressure ratio $n = p/p_n$, the Mach number M at the nozzle exit, and the ratio of specific heats γ. It is assumed in the paper that p and M are the flow parameters in the nozzle-exit section in the vicinity of the nozzle lip (point A in Fig. 1); p_n is the ambient pressure. The shock-wave intensity is $J = p_n/p = 1/n$. The maximum value of J ($J_{\max} = (1+\varepsilon)\mathrm{M}^2 - \varepsilon$, where $\varepsilon = (\gamma-1)/(\gamma+1)$) corresponds to the normal shock in the exit cross section and determines the lower boundary of the theoretically possible jet pressure ratio $n_{\max} < n < 1$ ($n_{\max} = 1/J_{\max}$).

The flow behind the incident shock AT is supersonic for $n_* < n < 1$ and subsonic for $n_{\max} < n < n_*$, where $n_* = 1/J_*$, and the special intensity

$$J_*(\mathrm{M}) = \frac{\mathrm{M}^2-1}{2} + \sqrt{\Big(\frac{\mathrm{M}^2-1}{2}\Big)^2 + \varepsilon(\mathrm{M}^2-1)+1}$$

corresponds to deceleration of the flow with the Mach number M to the critical velocity behind the shock wave. The following values of intensities are also called special [7, 8]:

Baltic State Technical University "Voenmekh," St. Petersburg 190005; uskov@peterlink.ru; mvcher@newmail.ru. Translated from Prikladnaya Mekhanika i Tekhnicheskaya Fizika, Vol. 47, No. 3, pp. 72–83, May–June, 2006. Original article submitted November 26, 2004; revision submitted August 17, 2005.

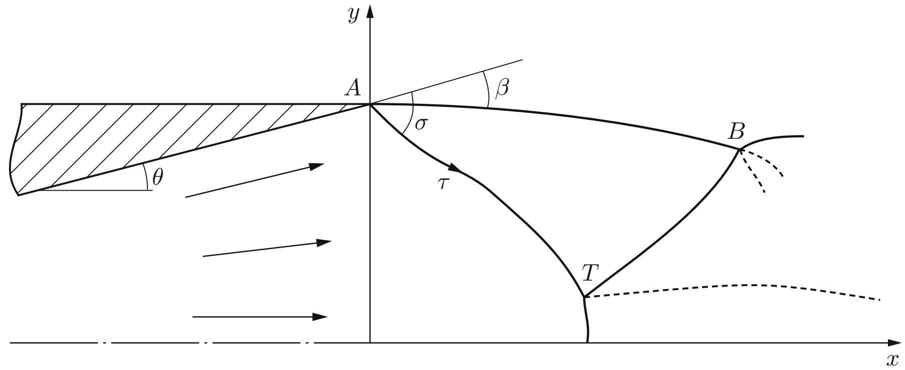

Fig. 1. Schematic of the flow of a plane overexpanded jet within the “first barrel.”

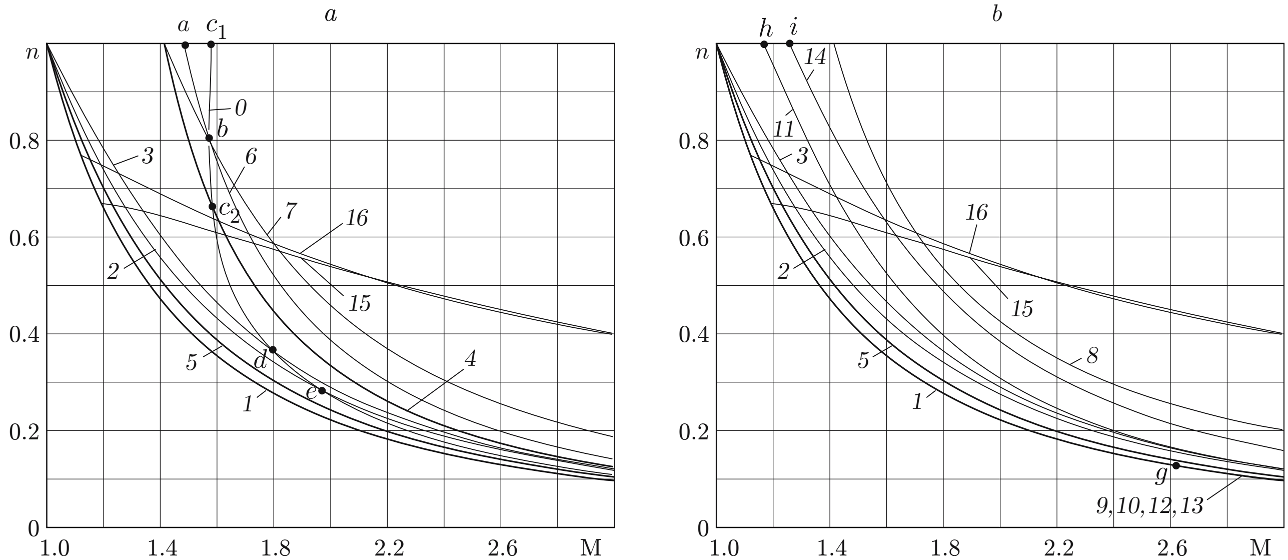

Fig. 2. Jet pressure ratios that refer to the special points of the shock wave (a) and to the jet boundary and the flow behind the shock (b) in the vicinity of the nozzle lip.

$$J_l(\mathrm{M}) = \frac{\mathrm{M}^2 - 2}{2} + \sqrt{\left(\frac{\mathrm{M}^2 - 2}{2}\right)^2 + (1 + 2\varepsilon)(\mathrm{M}^2 - 1) + 2}, \qquad J_\Gamma(\mathrm{M}) = \mathrm{M}^2 - 1. \tag{1}$$

The first of them determines the shock wave deflecting the flow to the greatest angle $\beta(\mathrm{M}, J, \gamma)$ with a fixed Mach number ahead of this shock, and the second expression determines the intensity of the shock wave deflecting the flow to the maximum angle, as compared to all other shock waves of an identical intensity (with different Mach numbers ahead of these shocks). Special intensities correspond to the jet pressure ratios $n_l = 1/J_l$ and $n_\Gamma = 1/J_\Gamma$. For all $\mathrm{M} > 1$, the inequalities $1 < J_\Gamma < J_* < J_l < J_{\max}$ and, correspondingly, $n_{\max} < n_l < n_* < n_\Gamma < 1$ are satisfied.

The dependences $n_{\max}(\mathrm{M})$, $n_l(\mathrm{M})$, and $n_*(\mathrm{M})$ of an overexpanded jet on the Mach number ahead of the shock wave are shown by curves 1–3 in Fig. 2a and b, and the dependence $n_\Gamma(\mathrm{M})$ is plotted as curve 4 in Fig. 2a.

The derivatives of various gas-dynamic variables of the jet flow suffer a discontinuity on the incident shock and are related by local differential conditions of compatibility [7] in the form

$$N_{i2} = C_i \sum_{j=1}^{4} A_{ij} N_j \qquad (i = 1, \ldots, 3), \tag{2}$$

where N_{i2} and N_j are the nonuniformities of the flow behind and ahead of the shock wave, respectively; the coefficients C_i and A_{ij} depend on M, J, and θ. The nonuniformities $N_1 = \partial \ln p/\partial s$, $N_2 = \partial\theta/\partial s$, and $N_3 = \partial \ln p_0/\partial n$ characterize the nonisobaricity, the curvature of streamlines, and the vorticity of the flow with a constant total heat; $N_4 \equiv K_\sigma$ is the shock-wave curvature. Conditions (2) determine the nonuniformities of the flow in the compressed layer immediately behind the shock of curvature found if the flow field ahead of the shock wave is known.

The condition of isobaricity of the flow ($N_{12} = 0$) along the free surface (jet boundary) AB (see Fig. 1) determines the sought curvature of the shock

$$K_\sigma = -\frac{1}{A_{14}} \sum_{j=1}^{3} A_{1j} N_j, \tag{3}$$

which affects the curvature $N_{22} \equiv K_\tau$ of the jet boundary:

$$K_\tau = \frac{C_2}{A_{15}} \sum_{j=1}^{3} (A_{2j} A_{14} - A_{1j} A_{24}) N_j.$$

Dependence (3), equations of motion of a two-dimensional gas flow ahead of and behind the shock in the "natural" coordinate system (s, n)

$$\frac{\mathrm{M}^2 - 1}{\gamma \mathrm{M}^2} N_1 + \frac{\partial\theta}{\partial n} + N_4 \sin\theta = 0, \qquad \gamma \mathrm{M}^2 N_2 = -\frac{\partial \ln p}{\partial n}, \qquad \frac{\partial p_0}{\partial s} = 0,$$

and the known relations between the shock-wave shape and intensity and Mach numbers on both sides of the shock [7]

$$J = (1 + \varepsilon)\mathrm{M}^2 \sin^2\sigma - \varepsilon,$$

$$\tan\ |\beta| = \sqrt{\frac{J_{\max} - J}{J + \varepsilon}}\, \frac{(1 - \varepsilon)(J - 1)}{J_{\max} + \varepsilon - (1 - \varepsilon)(J - 1)}, \qquad \mathrm{M}_2 = \sqrt{\frac{(J + \varepsilon)\mathrm{M}^2 - (1 - \varepsilon)(J^2 - 1)}{J(1 + \varepsilon J)}}$$

(σ is the angle between the shock wave and the flow velocity vector ahead of the shock wave) determine, after some transformations, the local changes in intensity and Mach number behind the shock in the direction τ along the shock wave:

$$\begin{aligned} \frac{dJ}{d\tau} &= -2(J + \varepsilon)(A_1 N_1 + A_2 N_2 + A_3 N_3 + q K_\sigma), \\ \frac{d\mathrm{M}_2}{d\tau} &= -[1 + \varepsilon(\mathrm{M}_2^2 - 1)]\Big(\frac{\mathrm{M}_2 N_{22}}{1 - \varepsilon} + \frac{N_{32}}{(1 + \varepsilon)\mathrm{M}_2}\Big) \sin(\sigma - \beta). \end{aligned} \tag{4}$$

Here $c = \sqrt{(J + \varepsilon)/(J_{\max} + \varepsilon)}$, $q = \sqrt{(J_{\max} - J)/(J + \varepsilon)}$, $A_1 = s[1 - (1 - 2\varepsilon)(\mathrm{M}^2 - 1)]/[(1 + \varepsilon)\mathrm{M}^2]$, $s = \sqrt{(J_{\max} - J)/(J_{\max} + \varepsilon)}$, $A_2 = c[(1 + \varepsilon(\mathrm{M}^2 - 1))/(1 - \varepsilon) - q^2]$, and $A_3 = c[1 + \varepsilon(\mathrm{M}^2 - 1)]/(J_{\max} + \varepsilon)$.

Curvature of the Shock Wave in a Plane Overexpanded Jet. Let, for certainty, the parameters of an isentropic flow ahead of the incident shock be described by the model of a cylindrical source (see Fig. 1). This model is usually used to describe exhaustion from a wedge-shaped (with a half-angle $\theta > 0$) or, in a particular case, contoured ($\theta = 0$) nozzle. Differentiation of the known relations [9] allows us to find flow nonisobaricity ahead of the shock wave on the nozzle lip:

$$N_1 = -\gamma \mathrm{M}^2 \sin\theta / [(\mathrm{M}^2 - 1) r]$$

(r is the distance from the nozzle lip to the plane of symmetry). As the streamlines are straight and there is no vorticity, we have $N_2 = N_3 = 0$. Relation (3) makes it possible to analyze the influence of the problem parameters M, n, γ, and θ on the specific features of the flow field in the vicinity of the nozzle lip. In particular, the shock-wave curvature depends monotonically on the nozzle half-angle (is proportional to $\sin\theta$). In all further calculations, we consider the dimensionless curvature $K_\sigma^- = r K_\sigma / \sin\theta$ and the ratio of specific heats $\gamma = 1.4$.

At low Mach numbers, the value of K_σ^- is positive (the shock wave AT in Fig. 1 is downward convex in the vicinity of the nozzle lip) and increases as a function of shock-wave intensity in the interval $(1; J_p)$, tending to infinity as $J \to J_p$ (Fig. 3a). The intensity $J_p(\mathrm{M}) \in (J_l; J_{\max})$ (the so-called constant-pressure point) is found from

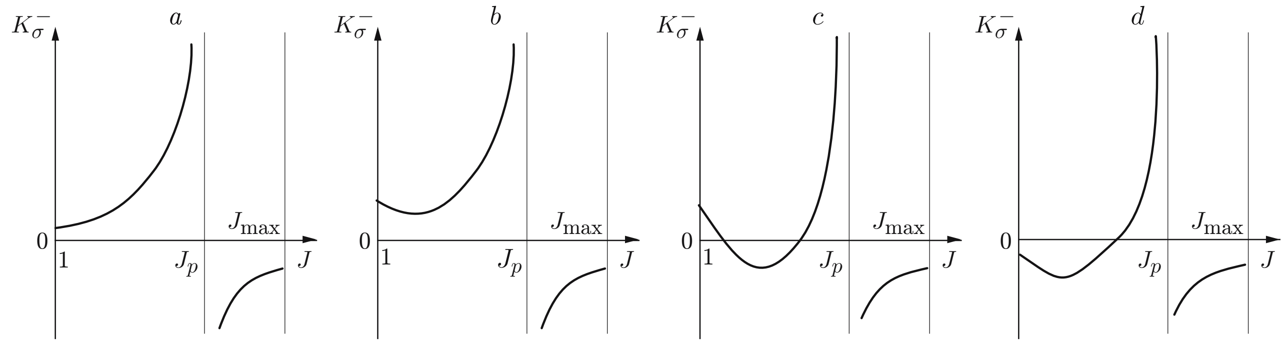

Fig. 3. Curvature of the incident shock wave versus its intensity: $\mathrm{M} < \mathrm{M}_a$ (a), $\mathrm{M}_a < \mathrm{M} < \mathrm{M}_b$ (b), $\mathrm{M}_b < \mathrm{M} < \mathrm{M}_c$ (c), and $\mathrm{M} > \mathrm{M}_c$ (d).

the condition $A_{14} = 0$ and always corresponds to a subsonic flow behind the incident shock. The corresponding jet pressure ratio $n_p = 1/J_p$ is shown by curve 5 in Fig. 2. For $J > J_p$, the curvature is negative. For all special values of intensity other than J_p, the shock-wave curvature is finite. In particular, as $J \to 1$ (degeneration into a weak discontinuity), as $J \to J_{\max}$ (normal shock), and at $J = J_\Gamma(\mathrm{M})$, it equals

$$\lim_{J\to 1} K_\sigma^- = -\frac{(1-2\varepsilon)\mathrm{M}^2 - 2(1-\varepsilon)}{(1-\varepsilon)\mathrm{M}(\mathrm{M}^2-1)}, \qquad \lim_{J\to J_{\max}} K_\sigma^- = -\frac{\mathrm{M}^2}{(1-\varepsilon)(\mathrm{M}^2-1)},$$

$$\lim_{J\to J_\Gamma} K_\sigma^- = -\frac{[(1-2\varepsilon)\mathrm{M}^2 - 2(1-\varepsilon)]\sqrt{\mathrm{M}^2-1+\varepsilon}}{(1-\varepsilon)\sqrt{1+\varepsilon}\,\mathrm{M}(\mathrm{M}^2-1)}.$$

As the Mach number increases to $\mathrm{M}_a = \sqrt{(2-\varepsilon)/(1-\varepsilon)} = 1.483$, there arises a minimum curvature (Fig. 3b), first, at the point $J = 1$. The jet pressure ratio $n_{\min} = 1/J_{\min}$ corresponding to the minimum shock-wave curvature is plotted by curve 6 in Fig. 2a. The value of the shock-wave curvature at the minimum point decreases to zero at a Mach number $\mathrm{M}_b = 1.571$ and intensity $J_b = 1.242$ and then becomes negative (Fig. 3c). For an arbitrary ratio of specific heats, the values of M_b and J_b are the greatest real roots of the equations

$$(3-4\varepsilon)^2\mathrm{M}_b^8 - 8(3-6\varepsilon+4\varepsilon^2)\mathrm{M}_b^6 + 8(1-3\varepsilon+4\varepsilon^2)\mathrm{M}_b^4 + 32\varepsilon(1-\varepsilon)\mathrm{M}_b^2 + 16(1-\varepsilon)^2 = 0,$$

$$\sum_{k=0}^{4} a_k J_b^k = 0,$$

$$a_4 = (1-\varepsilon)(3-4\varepsilon)(3+5\varepsilon), \qquad a_3 = -4(1-\varepsilon)(6+\varepsilon-3\varepsilon^2+16\varepsilon^3),$$

$$a_2 = -2(7+36\varepsilon-45\varepsilon^2-94\varepsilon^3+32\varepsilon^4-32\varepsilon^5), \quad a_1 = 4(4+11\varepsilon+6\varepsilon^2+39\varepsilon^3+52\varepsilon^4-16\varepsilon^5),$$

$$a_0 = 13+62\varepsilon+85\varepsilon^2-16\varepsilon^4+48\varepsilon^5.$$

Curve 0 in Fig. 2a determines the jet pressure ratios at which a shock wave of zero curvature emanates from the nozzle lip.

At a Mach number $\mathrm{M}_c = \sqrt{2(1-\varepsilon)/(1-2\varepsilon)} = 1.581$, the curvature of the shock wave degenerating into a weak discontinuity becomes negative for the first time (point c_1 in Fig. 2a). Another value of intensity of the shock wave of zero curvature at the same Mach number is $J_\Gamma(\mathrm{M}_c) = 1/(1-2\varepsilon) = 1.5$ and corresponds to the point c_2 in Fig. 2a. At $\mathrm{M} > \mathrm{M}_c$, the intensity of the shock wave of zero curvature rapidly increases (curve 0 in Fig. 2a) and reaches the value $J_d = J_*(\mathrm{M}_d) = 2.699$ for $\mathrm{M}_d = 1.787$. The flow behind the shock wave, which is straight in the vicinity of the nozzle lip, becomes subsonic. The Mach number M_d and intensity J_d are the greatest real roots of the equations

$$2(1-4\varepsilon)(1-2\varepsilon)\mathrm{M}_d^6 - (17-73\varepsilon+96\varepsilon^2-64\varepsilon^3)\mathrm{M}_d^4 + 4(1-\varepsilon)(9-24\varepsilon+32\varepsilon^2)\mathrm{M}_d^2 - 16(1-4\varepsilon)(1-\varepsilon)^2 = 0,$$

$$2(1-2\varepsilon)J_d^3 - (1+\varepsilon+8\varepsilon^2)J_d^2 - (3+5\varepsilon)J_d - (1-\varepsilon)(1+3\varepsilon) = 0.$$

At the Mach number $M_e = 1.974$, the point of zero curvature reaches a value $J_e = J_l(M_e) = 3.549$ and M_e and J_e being the greatest roots of the equations

$$(1-2\varepsilon)M_e^6 - (1+7\varepsilon-16\varepsilon^2+16\varepsilon^3)M_e^4 - 8(1-\varepsilon)(1-3\varepsilon+4\varepsilon^2)M_e^2 + 8(1-2\varepsilon)(1-\varepsilon)^2 = 0,$$

$$(1-2\varepsilon)J_e^3 - \varepsilon(3+4\varepsilon)J_e^2 - (5+2\varepsilon+4\varepsilon^2)J_e - (2+5\varepsilon-2\varepsilon^2) = 0.$$

In the limit ($M \to \infty$), the values of curvature of special shocks are negative

$$\lim_{\substack{J=J_\Gamma \\ M\to\infty}} K_\sigma^- = \lim_{\substack{J=J_* \\ M\to\infty}} K_\sigma^- = \lim_{\substack{J=J_l \\ M\to\infty}} K_\sigma^- = -\frac{1-2\varepsilon}{(1-\varepsilon)\sqrt{1+\varepsilon}},$$

$$\lim_{\substack{J=J_{\max} \\ M\to\infty}} K_\sigma^- = -\frac{1}{1-\varepsilon} = -1.2,$$

and it is only the curvature of the shock wave degenerating into a weak discontinuity ($J \to 1$) that tends to zero. The intensity of the shock wave of zero curvature tends to infinity; hence, we obtain

$$\lim_{M\to\infty} \frac{J}{M^2} = \frac{3-\varepsilon-4\varepsilon^2}{3(1-\varepsilon)} = 1.089.$$

At high Mach numbers, the special intensities of the shock waves are such that

$$\lim_{M\to\infty} \frac{J_\Gamma}{M^2} = \lim_{M\to\infty} \frac{J_*}{M^2} = \lim_{M\to\infty} \frac{J_l}{M^2} = 1, \qquad \lim_{M\to\infty} \frac{J_p}{M^2} = \frac{3(1+\varepsilon)}{3+\varepsilon} = 1.105.$$

The point of zero curvature at high Mach numbers corresponds to a strong shock wave with a subsonic flow behind the latter.

The intensity $J_{\min}$ of the shock wave of minimum curvature, vice versa, corresponds to a supersonic flow in the compressed layer (see curve 6 in Fig. 2a), At high Mach numbers, it is described by the relation

$$\lim_{M\to\infty} \frac{J_{\min}}{M^2} = \frac{(1+\varepsilon)(9+9\varepsilon+2\varepsilon^2-2\varepsilon\sqrt{18-18\varepsilon+\varepsilon^2}\,)}{3(3-2\varepsilon-\varepsilon^2)} = 0.913,$$

and the dimensionless curvature of this shock tends to the value

$$\lim_{\substack{J=J_{\min} \\ M\to\infty}} K_\sigma^- = \sqrt{\frac{81-243\varepsilon+333\varepsilon^2-261\varepsilon^3+88\varepsilon^4+2\varepsilon^5-Q}{3(3+\varepsilon)^3(1-\varepsilon)^3}} = -0.767,$$

$$Q = 2\varepsilon(1-\varepsilon)(18-18\varepsilon+\varepsilon^2)^{3/2}.$$

Changes in Intensity of the Incident Shock Wave in the Vicinity of the Nozzle Lip. The change in shock-wave intensity in the vicinity of the nozzle lip is described by the derivative $dJ/d\tau$ [see (4)] in the direction downstream from the lip. An analysis of this quantity is necessary to describe the flow in the compressed layer, because the shock-wave intensity unambiguously determines the total pressure losses and the increase in entropy of the gas on the shock wave:

$$I = p_{02}/p_0 = (J\Omega^\gamma)^{-(1-\varepsilon)/(2\varepsilon)}, \qquad \Delta S = c_v \ln(J\Omega^\gamma). \tag{5}$$

Here c_v is the heat capacity at constant volume and $\Omega = (1+\varepsilon J)/(J+\varepsilon)$ is the ratio of specific volumes behind and ahead of the shock in accordance with the Rankine–Hugoniot shock adiabat. Hence, the derivative $dJ/d\tau$ shows the direction of variation of the total pressure and the increase in entropy of the gas in passing from one streamline to another in the compressed layer; a similar derivative of entropy proportional to $dJ/d\tau$ characterizes the absolute value of the velocity vorticity vector in the compressed layer.

According to Eq. (4), the derivative $dJ/d\tau$ is proportional to $\sin\theta/r$ in the model of the flow from a source. In particular, the intensity of a straight shock wave in a uniform flow with $\theta = 0$ remains unchanged until the reflection point. In what follows, we consider the dimensionless quantity $W_J = (r/\sin\theta)\, dJ/d\tau$ independent of the radius of the nozzle-exit cross section and of the nozzle half-angle.

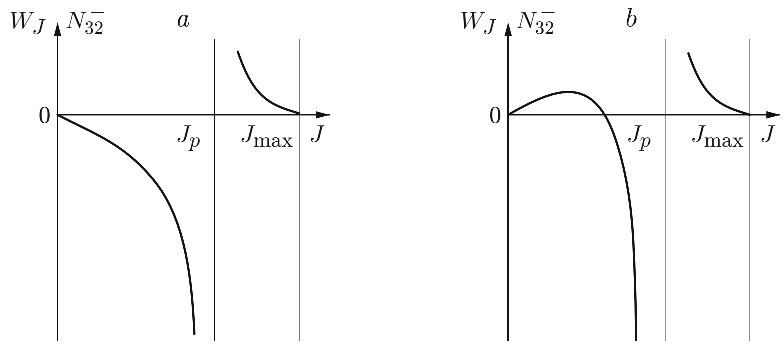

Fig. 4. Dependences $W_J(J)$ and $N_{32}^-(J)$ for $\mathrm{M} < \sqrt{2}$ (a) and $\mathrm{M} > \sqrt{2}$ (b).

The dimensionless derivative W_J equals zero (Fig. 4) both in the case of formation of the normal shock ($J = J_{\max}$) and in the case of degeneration of the shock wave into a weak discontinuity ($J \to 1$). The latter indicates the transition from the shock attached to the nozzle lip to a detached shock at a certain distance from the nozzle lip as the overexpansion transforms to an isobaric flow.

For $\mathrm{M} < \sqrt{2}$, the value of W_J is negative and monotonically decreases in the interval $(1; J_p)$ tending to an infinite value as $J \to J_p$ (Fig. 4a). Hence, the shock waves formed in an overexpanded jet with $\mathrm{M} < \sqrt{2}$ have a tendency to attenuation when approaching the plane of symmetry. In the interval $(J_p; J_{\max})$, vice versa, they are amplified and tend to become normal shocks on the plane of symmetry.

For $\mathrm{M} > \sqrt{2}$ and small or moderate intensity of the shock, the derivative is $dJ/d\tau > 0$ (Fig. 4b); hence, these shock waves are amplified in the vicinity of the nozzle lip. The shock waves with the zero value of the derivative $dJ/d\tau$ are described by Eq. (1). The intensity of shock waves satisfying the inequality $J_\Gamma < J < J_p$ still decreases with distance from the nozzle lip. As the intensity J_* corresponding to the critical flow behind the shock satisfies this inequality ($J_\Gamma < J_* < J_p$), the flow behind the attenuating shock can be either supersonic or subsonic. The behavior of strong ($J > J_p$) shock waves remains unchanged with variation of the Mach number.

The maximum values of the function W_J in the interval $(1; J_\Gamma)$ correspond to shock waves with the maximum growth rates of intensity in the vicinity of the nozzle lip. The jet pressure ratios $n = 1/J$ in jets with the most rapidly amplified shock waves are shown by curve 7 in Fig. 2a. At high Mach numbers, the intensities of these shocks and their derivatives W_J tend to infinitely high (of the order of M^2) values and are characterized by the relations

$$\lim_{\mathrm{M}\to\infty} \frac{J}{\mathrm{M}^2} = L_1, \qquad \lim_{\mathrm{M}\to\infty} \frac{W_J}{\mathrm{M}^2} = 0.098,$$

where $L_1 = 0.638$ is the unique real root of the equation

$$3(3+\varepsilon)L_1^3 - 2(12+12\varepsilon+\varepsilon^2)L_1^2 + 3(1+\varepsilon)(7+4\varepsilon)L_1 - 6(1+\varepsilon)^2 = 0.$$

The flow behind the shock waves with the highest growth rate of intensity is supersonic.

Thus, curves 4 [$n = n_\Gamma(\mathrm{M})$] and 5 [$n = n_p(\mathrm{M})$] in Fig. 2a separate the ranges of jet pressure ratios of an overexpanded jet in which the shock wave arriving at the plane of symmetry is amplified or (in the region between these curves) attenuated. For $\mathrm{M} < \sqrt{2}$, the shock waves emanating from the nozzle lip are attenuated for all jet pressure ratios in the interval $n_p < n < 1$ that can be encountered in practice. The calculation by the method of characteristics [10] performed for jets with $n = 0.8$ ($J = 1.25$), $\theta = 15^\circ$, and different Mach numbers of the exhausting jet shows that the smaller the Mach number, the longer the interval of the shock-wave intensity decrease. For a Mach number (in our case, $\mathrm{M} = 1.5$) satisfying Eq. (1), the shock-wave intensity monotonically increases up to the plane of symmetry.

A change in the ratio of specific heats of the gas does not induce any qualitative changes in the solution of the problem of the shock-wave intensity derivative.

Extreme Values of Flow Vorticity. As it follows from relation (5), the total pressure losses on the shock with a fixed value of γ is a function of the shock-wave intensity only. The total pressure gradient

$$N_{32} = \frac{\partial \ln p_0}{\partial n} = \frac{(1-\varepsilon)(J-1)^2\sqrt{(J_{\max}-J)(J+\varepsilon)+(1+\varepsilon J)^2}}{2J(J+\varepsilon)(1+\varepsilon J)^2}\,\frac{dJ}{d\tau},$$

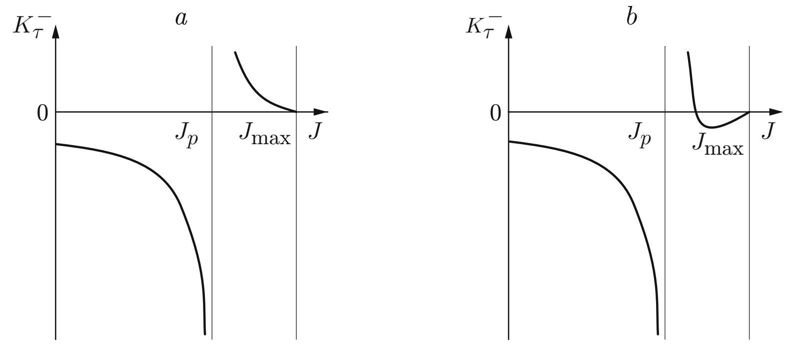

Fig. 5. Curvature of the jet boundary for $M < M_g$ (a) and $M > M_g$ (b).

which shows the change in flow vorticity, has the same sign as the function $W_J(M, J)$ considered above. As the jet pressure ratio changes, the flow vorticity exerts the behavior illustrated in Fig. 4. If a supersonic jet is close to the isobaric state ($J \to 1$), flow vorticity is very low. Zero values of flow vorticity are observed behind the normal shock ($J = J_{\max}$) and only at one point: root of the function $W_J(J)$ in the interval $J \in (1; J_p)$ for $M < \sqrt{2}$.

The extreme points of the function $N_{32}^-(J) = rN_{32}/\sin\theta$ are observed for $M > \sqrt{2}$. For $M < 2.569$, in contrast to the extreme points of the function $W_J(J)$, these points correspond to higher intensities of the incident shock (and lower jet pressure ratios). The extreme points of two functions coincide only at one combination of the Mach number and jet pressure ratio ($M = 2.569$ and $J = 3.825$), and the maximum flow vorticity is further reached with lower shock-wave intensities (curve 8 in Fig. 2b).

The jet parameters corresponding to the extreme values of vorticity are found by solving algebraic equations of the eighth power in terms of the jet pressure ratio and of the fourth power with respect to the square of the jet Mach number in the vicinity of the nozzle lip. The values of vorticity N_{32}^- tend to zero at the special points $J_*(M)$, $J_\Gamma(M)$, and $J_l(M)$ as $M \to \infty$. At the extreme point corresponding to the intensity $J \approx M^2$ at high Mach numbers, the dimensionless vorticity in the compressed layer tends to $A = 26.670$, which is the root of the equation

$$3\varepsilon A^4 - (9 + 22\varepsilon - 22\varepsilon^2)A^3 - (14 + 31\varepsilon + 44\varepsilon^2)A^2 - (1 + 20\varepsilon + 22\varepsilon^2 + 24\varepsilon^3)A - 2\varepsilon(1 + 4\varepsilon) = 0.$$

Curvature of the Boundary of an Overexpanded Jet. The jet boundary in the vicinity of the nozzle lip is normally upward convex (see, e.g., Fig. 1). The dimensionless curvature $K_\tau^-(M, J) = rK_\tau/\sin\theta$ becomes negative, in particular, in the case of incidence of a weak shock wave

$$\lim_{J\to 1} K_\tau^-(M, J) = -1/\sqrt{M^2 - 1},$$

which is also supported by the conclusions made from the conditions of compatibility on a weak discontinuity [7]. In the limit ($M \to \infty$), the curvature of the jet boundary behind a weak shock wave tends to zero; at the special points $J_*(M)$, $J_\Gamma(M)$, and $J_l(M)$, it tends to -1. Exceptions are cases of very strong overexpansion (regions on the right of the infinite discontinuity of curvature at $J = J_p$ in Fig. 5). In particular, the curvature of the boundary equals zero behind the normal shock [at $J = J_{\max}(M)$]; it is positive at low Mach numbers in the interval $J \in (J_p; J_{\max})$ and has a root at $M > M_g$, where $M_g = \sqrt{(4 - 3\varepsilon)/(1 - 3\varepsilon)} = 2.646$. The zero values of curvature of the jet boundary are described by the relation (curve 9 in Fig. 2b)

$$M = \sqrt{\frac{3(1-\varepsilon)J^3 + 2(3 + \varepsilon - 2\varepsilon^2)J^2 - (5 - 13\varepsilon)J - 4\varepsilon(1 - 2\varepsilon) + \sqrt{D}}{2[(3-\varepsilon)J^2 + (1 + 9\varepsilon)J + 4\varepsilon^2]}},$$

$$D = 9(1-\varepsilon)^2J^6 - 4(1-\varepsilon)(3 - 7\varepsilon + 6\varepsilon^2)J^5 - 2(5 + 22\varepsilon - 43\varepsilon^2 + 16\varepsilon^3 - 8\varepsilon^4)J^4$$
$$- 4(3 - 8\varepsilon + 3\varepsilon^2 - 14\varepsilon^3)J^3 + (41 - 2\varepsilon + 41\varepsilon^2 + 16\varepsilon^3)J^2 + 8\varepsilon(7 + \varepsilon)J + 16\varepsilon^2$$

and obey the law

$$\lim_{M\to\infty} \frac{J}{M^2} = \frac{3 - \varepsilon}{3(1 - \varepsilon)} = 1.133.$$

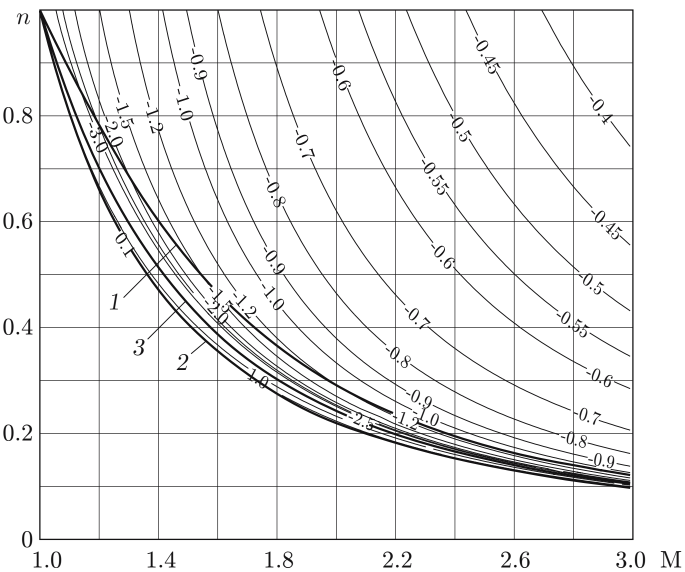

Fig. 6. Isolines of the dimensionless curvature $K_\tau^- = rK_\tau/\sin\theta$.

The curvature K_τ^- at the minimum point has a finite limit as $\mathrm{M} \to \infty$ ($K_\tau^- \to -0.207$), and the shock-wave intensity at this point is such that $J/\mathrm{M}^2 \to C$, where the value $C = 1.153$ is determined by the equation

$$\sum_{k=0}^{4} H_k C^k = 0,$$

$$H_4 = 3(3+\varepsilon)(1-\varepsilon)^2, \qquad H_3 = -2(1-\varepsilon)(18+3\varepsilon-13\varepsilon^2),$$

$$H_2 = 2(1-\varepsilon^2)(27-8\varepsilon^2), \quad H_1 = -2(1+\varepsilon)(18-3\varepsilon-13\varepsilon^2), \quad H_0 = 3(3-\varepsilon)(1+\varepsilon^2).$$

The minimums and the zero values of curvature of the jet boundary for $J \in (J_p; J_{\max}]$ are shown as curves 9 and 10 in Fig. 2b, respectively, which almost merge with curve 1 corresponding to normal shocks.

The curvature of the boundary is an important parameter affecting the development of the Taylor–Görtler instability. It is seen from Fig. 6 that the dimensionless curvature K_τ^- significantly depends on the Mach number, decreasing in absolute value with increasing Mach number. The transition to a subsonic flow behind the shock [$n = n_*(\mathrm{M})$; curve 1] does not affect the curvature of the boundary, and an infinite discontinuity occurs at $n = n_p(\mathrm{M})$. If the exhaustion with $n \in (n_{\max}(\mathrm{M}); n_p(\mathrm{M}))$ (region between curves 2 and 3) does occur, a small fluctuation of the jet pressure ratio seems to be able to significantly distort its boundary.

Change in Static Pressure behind the Shock Wave. The derivative of static pressure $P_w = (\partial \ln p/\partial\tau)\,(r/\sin\theta)$ behind the shock is determined, first, by the decrease in pressure ahead of the shock wave as the latter moves away from the nozzle lip and, second, by a possible increase in shock-wave intensity and the corresponding increase in pressure behind the shock. The function $P_w(\mathrm{M}, J)$ is determined by two terms

$$P_w(\mathrm{M}, J) = -\sqrt{\frac{J_{\max} - J}{J_{\max} + \varepsilon}}\,\frac{\gamma \mathrm{M}^2}{\mathrm{M}^2 - 1} + \frac{1}{J}\,W_J(\mathrm{M}, J),$$

each describing the effect of one factor. In particular, as $J \to 1$ ($W_J \equiv 0$), the pressure behind a weak shock wave decreases as

$$P_w(\mathrm{M}, J = 1) = -\gamma \mathrm{M}/\sqrt{\mathrm{M}^2 - 1};$$

this decrease is especially pronounced at low Mach numbers. Behind the normal shock, we have $P_w(\mathrm{M}, J_{\max}) = 0$.

At low Mach numbers (Fig. 7a and b), the function P_w is rigorously negative for all $J \in [1; J_p)$, i.e., in all cases of shock-wave shedding directly from the lip, which are encountered in practice, and is non-negative in the interval $(J_p; J_{\max}]$. For a Mach number

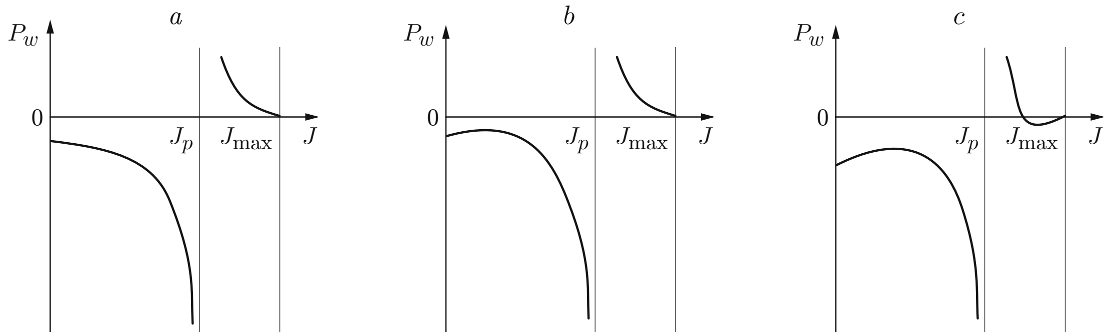

Fig. 7. Derivative of static pressure for $\mathrm{M} < \mathrm{M}_h$ (a), $\mathrm{M}_h < \mathrm{M} < \mathrm{M}_g$ (b), and $\mathrm{M} > \mathrm{M}_g$ (c).

$$\mathrm{M}_h = \sqrt{\Big(\sqrt{9 - 4\varepsilon + 4\varepsilon^2} - 3 + 6\varepsilon\Big)/(4\varepsilon)} = 1.166,$$

the function $P_w(J)$ has a maximum (Fig. 7b). Curve 11 in Fig. 2b shows the jet pressure ratio at the point of this maximum. The derivative of pressure at the maximum point is still negative and tends to -0.519 as $\mathrm{M} \to \infty$. Hence, the static pressure in the compressed layer of the jet behind the shock wave normally decreases.

For $\mathrm{M} = \mathrm{M}_g = \sqrt{(4 - 3\varepsilon)/(1 - 3\varepsilon)} = 2.646$, a second extreme point of the function P_w is formed: it lies in the region of high intensities (Fig. 7c). The function of pressure at the new minimum point tends to -0.050 as $\mathrm{M} \to \infty$. At high Mach numbers, the extreme points are determined by the limits

$$\lim_{\mathrm{M}\to\infty} \frac{J}{\mathrm{M}^2} = C_{1,2}, \qquad C_{1,2} = \frac{9 - 13\varepsilon \mp 4\varepsilon\sqrt{\varepsilon(3 + \varepsilon - 3\varepsilon^2)}}{3(3 - 2\varepsilon + \varepsilon^2)}$$

($C_1 = 1.030$ and $C_2 = 1.151$). Thus, the shock-wave intensity at the first extreme point, which is equal to unity at $\mathrm{M} = \mathrm{M}_h$, becomes slightly higher than $J_*(\mathrm{M})$, $J_\Gamma(\mathrm{M})$, and $J_l(\mathrm{M})$ at high Mach numbers. The function P_w tends to the same value $(-\sqrt{\varepsilon(1+\varepsilon)}/(1-\varepsilon) = -0.529)$ at all these special points as $\mathrm{M} \to \infty$. Curves 12 and 13 in Fig. 2b, which show the values of the found minimums and roots of the function $P_w(J)$ in strongly overexpanded jets almost merge with curves 9 and 10, which show the specific properties of the curvature of the jet boundary, and with curve 1 corresponding to the normal shock. For $\gamma > 2$ ($\varepsilon > 1/3$), the second extreme point is not formed.

Change in the Mach Number in the Compressed Layer. The change in the Mach number in the compressed layer behind the shock wave is also induced by two factors: gas expansion ahead of the shock and, hence, an increase in the Mach number as the shock moves away from the nozzle lip, on one hand, and a possible increase in shock-wave intensity with a corresponding decrease in the Mach number behind the shock, on the other hand. Therefore, the conclusions of the previous Section are qualitatively valid for the description of changes in the Mach number in the compressed layer in an overexpanded jet as well.

As was found above, the shock-wave intensity in the vicinity of the nozzle lip at low Mach numbers either decreases or weakly increases. Therefore, the function $\mathrm{M}'_w(J)$ is negative for small M in the entire half-interval $[1; J_p)$ and experiences an infinite discontinuity as $J \to J_p$ (Fig. 8a). At the point $J = J_{\max}(\mathrm{M})$, the derivative is $\mathrm{M}'_w \equiv 0$.

For a Mach number

$$\mathrm{M}_i = \sqrt{\Big(6\varepsilon - 1 + \sqrt{1 + 20\varepsilon + 4\varepsilon^2}\Big)/(8\varepsilon)} = 1.257$$

there arises a local minimum of the function $\mathrm{M}'_w(J)$ at the point $J = 1$ (Fig. 8b). With increasing Mach number,

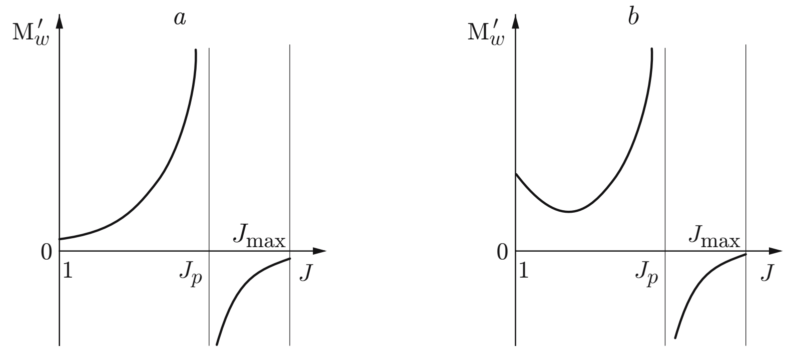

Fig. 8. Derivative of the Mach number behind the shock for $M < M_i$ (a) and $M > M_i$ (b).

the minimum point is shifted toward the increase in shock-wave intensity (curve 14 in Fig. 2b) and is described by the limit

$$\lim_{M\to\infty} \frac{J}{M^2} = D,$$

where $D = 0.641$ is the root of the equation

$$(3+\varepsilon)D^4 - 2(1-\varepsilon^2)(3-\varepsilon)(2+\varepsilon)D^3 + 2(1+\varepsilon)(9+5\varepsilon-8\varepsilon^2-2\varepsilon^3)D^2 - 6(2-\varepsilon)(1+\varepsilon)^3 D + 3(1+\varepsilon)^3 = 0.$$

In contrast to the cases $J \to 1$ and $J \to J_p$, the function M'_w at the point of its local minimum is finite even as $M \to \infty$ (its limit is 0.258 for $\gamma = 1.4$). The limiting values of the function M'_w for special shock-wave intensities are also finite:

$$\lim_{\substack{M\to\infty \\ J=J_\Gamma}} M'_w = \lim_{\substack{M\to\infty \\ J=J_*}} M'_w = \lim_{\substack{M\to\infty \\ J=J_l}} M'_w = \frac{\sqrt{\varepsilon}}{(1-\varepsilon)\sqrt{1+\varepsilon}} = 0.454.$$

Thus, the Mach number behind the shock wave emanating from the nozzle lip in a plane overexpanded jet increases as the jet moves away from the nozzle lip in all cases important for practice. This means, in particular, that the flow in the compressed layer, at least in the vicinity of the nozzle lip, is supersonic behind a shock wave of intensity $J_*(M)$, if the Mach number at the jet boundary becomes equal to unity.

According to the results of [7], a local decrease in static pressure and an increase in the Mach number behind the shock wave normally occur in axisymmetric overexpanded jets as well.

Additional Comment. Flow separation from the nozzle walls in an excessively overexpanded flow prevents the occurrence of the flow features described above. As was noted in [11], the critical intensity $J = 1/n$ of the shock wave causing separation of a turbulent boundary layer is estimated according to Nekrasov as

$$J = 1 + 0.2\gamma M^2 (M^2 - 1)^{-1/4}$$

or according to Gedd as

$$J = [(1 + 0.5(\gamma-1)M^2)/(1 + 0.32(\gamma-1)M^2)]^{\gamma/(\gamma-1)}.$$

Curves 15 and 16 in Fig. 2a and b corresponding to these jet pressure ratios show that some specific features of the flow usually do not occur at moderate Mach numbers. The majority of the indicated features (change in the direction of convexity of the shock wave, decrease in its intensity, etc.), however, correspond to the range of low Mach numbers, where flow separation occurs extremely rarely. In addition, the currently existing methods of boundary-layer suction shift the separation to the region of lower jet pressure ratios.

Conclusions. It was theoretically established that many parameters of an overexpanded jet in the vicinity of the nozzle lip acquire extreme values. This circumstance can be used to optimize jet flows and control their acoustic field, vortex formation, and flow separation.

This work was supported by the Russian Foundation for Basic Research (Grant No. 04-01-00713).

REFERENCES

1. V. N. Glaznev, V. I. Zapryagaev, V. N. Uskov, et al., *Jets and Unsteady Flows in Gas Dynamics* [in Russian], Izd. Sib. Otd. Ross. Akad. Nauk, Novosibirsk (2000).
2. N. M. Terekhova, "Streamwise vortices in axisymmetric jets," *Dokl. Ross. Akad. Nauk*, **347**, No. 6, 759–762 (1996).
3. N. M. Terekhova, "Dynamics of unstable oscillations in a supersonic jet," *J. Appl. Mech. Tech. Phys.*, **35**, No. 6, 817–822 (1994).
4. N. M. Terekhova, "Streamwise vortices in axisymmetric jets," *J. Appl. Mech. Tech. Phys.*, **37**, No. 3, 339–349 (1996).
5. V. I. Zapryagaev, N. P. Kiselev, and A. A. Pavlov, "Effect of streamline curvature on intensity of streamwise vortices in the mixing layer of supersonic jets," *J. Appl. Mech. Tech. Phys.*, **45**, No. 3, 335–434 (2004).
6. V. I. Zapryagaev, A. V. Solotchin, and N. P. Kiselev, "Structure of a supersonic jet with varied geometry of the nozzle entrance," *J. Appl. Mech. Tech. Phys.*, **43**, No. 4, 538–543 (2002).
7. A. L. Adrianov, A. L. Starykh, and V. N. Uskov, *Interference of Steady Gas-Dynamic Discontinuities* [in Russian], Nauka, Novosibirsk (1995).
8. V. N. Uskov, *Shock Waves and Their Interaction* [in Russian], Izd. Leningr. Mekh. Inst., Leningrad (1980).
9. V. S. Avduevskii, E. A. Ashratov, A. V. Ivanov, and U. G. Pirumov, *Gas-Dynamics of Supersonic Nonisobaric Jets* [in Russian], Mashinostroenie, Moscow (1989).
10. O. N. Katskova, I. N. Naumova, Yu. D. Shmyglevskii, and N. P. Shulinshina, *Experience of Calculating Plane and Axisymmetric Supersonic Gas Flows by the Method of Characteristics* [in Russian], Comput. Center, Acad. of Sci. of the USSR, Moscow (1961).
11. G. N. Abramovich, *Applied Gas Dynamics* [in Russian], Nauka, Moscow (1976).